Polyamides Nanocapsules: Modeling and Wall Thickness Estimation

K. Bouchemal, F. Couenne, S. Briançon, H. Fessi, and M. Tayakout
Laboratoire d'Automatique et de Génie des Procédés UMR-CNRS 5007, Université Claude Bernard Lyon, ESCPE BAT 308G, 43 Bd du 11 Novembre 1918, 69622 Villeurbanne, France

DOI 10.1002/aic.10828
Published online March 31, 2006 in Wiley InterScience (www.interscience.wiley.com).

This work provides a better understanding for effective control of the nanocapsules wall thickness. Polyamides based nanocapsules are prepared by interfacial polymerization combined with spontaneous emulsification. A clear guideline of how factors such as monomer concentration, diffusion, interfacial reaction, or water swelling influence the capsule formation is very important to the control of capsule wall structure and release performance. In this goal, the macroscopic planar models of the interfacial polycondensation between diethylenetriamine and sebacoyle chloride are studied experimentally and theoretically. This planar model is developed to examine the kinetics of the reaction and to perform the estimation of parameters thanks to the experiment measurements. The effect of the operating conditions on the wall thickness is also studied. The model is shown to be consistent with the experimental data. Next, the spherical model is deduced from the first one. The results obtained with this model are in accordance with some observations of wall thickness. From this model, the increase of the wall thickness is predicted for several operating conditions. © 2006 American Institute of Chemical Engineers *AIChE J,* 52: 2161–2170, 2006

Keywords: polyamide films, interfacial polycondensation, swelling, modeling, estimation

Introduction

Swellable polymers are considered as an attractive carrier for drug delivery systems. One of several methods to produce the wall of nanocapsule is interfacial polycondensation: the polymer wall is produced at the interface of two immiscible phases. The release of the capsule content depends strongly on many factors, such as the capsule wall thickness. So it is important to understand the phenomena that occur during the wall growth. The aim of this article is to propose a dynamical model of the interfacial polycondensation in order to predict the wall thickness of the capsule produced by this mechanism.

Liquid–liquid interfacial polymerization has been well studied. Morgan and co-workers[1-4] have presented a systematic study of the polycondensation of diacid chlorides with diamines. They have shown that the interfacial polymerization reaction taking place in the organic phase close to the interface between the aqueous and organic phases, involves an SN2 (bimolecular nucleophilic substitution) mechanism.[1-5] Kinetic studies of other systems, such as polyester formation, have also been reported.[6-8] Different models of microcapsules formation have been developed in the literature.[9-11]

More recently, the kinetic of encapsulation by the polycondensation of terephthaloyl dichloride (TDC) with diethylenetriamine (DETA) at the interface of an oil–water emulsion has been studied.[12-14] The developed diffusion controlled model is based on the mass balance of TDC over the capsule with the presence of two layers (one with a fixed thickness, the other one called d with a growing thickness). It is developed in a planar geometry. With adequate assumptions on the layers and on the DETA rate consumption in the capsule, the authors get a simple analytic formulation of the growth of d with respect to time. It turned out that this model incorrectly predicts the membrane thickness for long times.

Correspondence concerning this article should be addressed to F. Couenne at couenne@lagep.univ-lyon1.fr.

Finally, Ji and coworkers[15] presented a dynamic planar model for the film taking into account the diffusion and interfacial polymerization phenomena for the same polymerization reaction. They also extended this work to a cylindrical film[16] and to spherical geometry.[17] In these latter models, developments are based on the assumption of a linear concentration profile (first order development of the integral of the concentration along the radial coordinate of the capsule) leading to a simplified differential equation for the growth wall. Let us notice that the swelling is not explicitly accounted for.[15-17]

In this article, interfacial polymerization combined with spontaneous emulsification technique is studied. The physicochemical evaluation of a nanoparticulate drug carrier is technically difficult to achieve owing to the very small size (150-500nm) of the particles in the final colloidal suspension product. So the experimental part is developed for the planar geometry. The mathematical model is given first in the planar geometry and second in the spherical one since it appears that the basic morphology of the nanocapsules under consideration is a sphere. The main feature of the model is that all the main phenomena are taken into account: the swelling, the diffusion, and the interfacial polymerization. The swelling is not modeled in the previously quoted studies.[1-17]

The planar model will be used to understand the reaction of interfacial polycondensation and, thus, the physical phenomena brought into play because their dynamics are slower than in the spherical system. Taking into account -the parameters estimated on the macroscopic scale (planar model), the simulation of the spherical model gives qualitative and quantitative information on what occurs when the operating conditions are changed. Simulation results are then proposed and discussed for this second model.

Planar Model

Materials and methods

The manufacturing process of polyamides by interfacial film polycondensation consists of putting into contact an acid chloride solution in an inert and immiscible organic solvent with an aqueous phase of an amine. The formed polymer can be soluble, dispersed in one of the two phases, or insoluble. It depends on the used monomer as well as the used organic solvent. If the two phases put in contact are immiscible and if the organic solvent does not dissolve the polymer, a thin polymer film is formed at the interface. We find a combination that observes these conditions: the organic phase is composed of cyclohexane, of liposoluble monomer (sebacoyl chloride), and of liposoluble surfactant (Span® 85); and the aqueous phase is made of water, of triamine (DETA), and of surfactant Tween® 20. Monomers and solvents come from Sigma, France. Surfactants were supplied by Seppic France.

The experimental setup used for studying the kinetic of the polymerization reaction between the DETA and the sebacoyl chloride is represented in Figure 1. An organic phase (1) composed of 400 ml cyclohexane and 10^{-2} mol sebacoyl chloride is delicately poured (3) in an homogeneous solution of 10^{-1} mol diethylenetriamine in 800 ml water contained in a two liter reactor (2). The organic phase is homogenized by a magnetic stirring bar and the aqueous phase is homogenized with a mechanical stirrer. The reactor is closed to limit the cyclohexane evaporation.

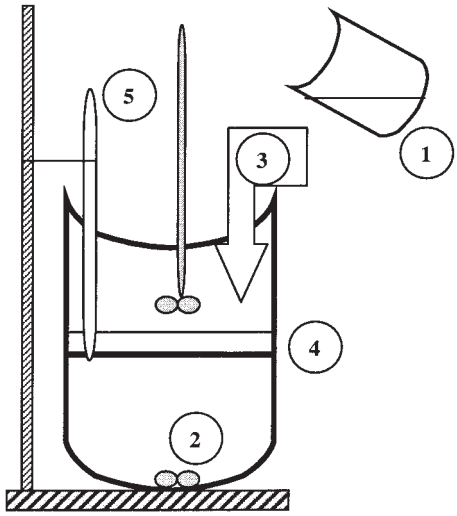

Figure 1. Scheme of the experimental setup.

1. Organic phase, 2. Aqueous phase, 3. Flow of the organic phase throughout the walls of the reactor, 4. Liquid-liquid interface, formation of the primary wall, 5. Thermometer.

The polymer film is formed instantaneously when the two phases are in contact (4). The temperature (5) of the system increases 1°C at this time. This stage corresponds to the formation of a transparent primary membrane. Within a few minutes, the film becomes opaque and the thickness does not cease growing until reaching a maximum thickness after several days of reaction.

We carry out a series of preparations. They are started at the same time but stopped at different times. At the end of each experiment, the monomers chloride sebacoyle and diethylenetriamine in each phase are assayed in the aim of plotting the concentrations curve versus time. The sebacoyl chloride and diethylenetriamine concentrations are obtained using infrared spectroscopy and basic acid titration, respectively.

At the end of each experiment, the polymer is washed with distilled water, slightly dried, and weighed on a precision balance (0.1 mg). The thickness of polymer is given by using a Mitutoyo gauge with 10μm accuracy. Measurements are done at several places. The result represents the average of these measurements in mm.

The formation of polymer film is due to the reaction between the monomers A (sebacoyl chloride) and B (diethylenetriamine). The monomer B, present in the aqueous phase, diffuses towards the organic phase. The monomer B reacts with monomer A by forming polymer and chloride acid denoted H:

$$\lambda_A A + \lambda_B B = \lambda_P \text{Polymer} + \lambda_H H \qquad \text{(R1)}$$

where λ_A, λ_B, λ_P, and λ_H are the stoichiometric coefficients of A, B, the polymer, and H, respectively. This reaction takes place in the organic phase of the liquid-liquid interface situated on the top of Figure 2. The reaction rate for the reaction (R1) is chosen as $r_1 = k_1 C_A^n C_B$.

The polymer membrane has a planar geometry. The internal section of the reactor is constant. When the reaction of polymerization starts, a planar polymer membrane is formed, the zone of reaction initially localized at $x = 0$ (Figure 2).

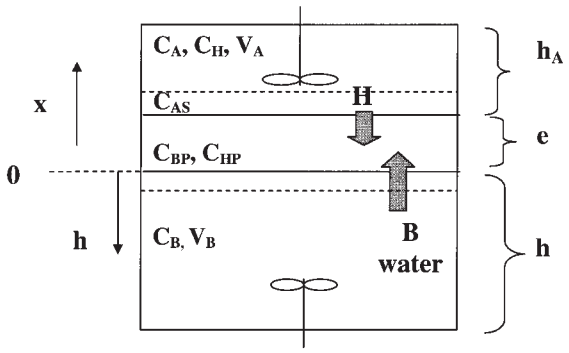

Figure 2. Diagram of the experiment.

The polymer wall thickness e results on the reaction (R1) and on the swelling due to water sorption represented by

$$\text{Polymer} + \text{Water} = [\text{polymer} - \text{water}] \qquad \text{(R2)}$$

In the polymer, the concentration of monomer B and of H is indexed by P: C_{BP} and C_{HP}.

Finally, the chloride acid (H), which diffuses through the membrane, reacts in the aqueous phase and in the polymer with the monomer B:

$$\lambda_H H + \lambda_B B = \lambda_B B\text{-protonic} \qquad \text{(R3)}$$

The reaction rate for the reaction (R3) is chosen as $r_3 = k_3 C_B C_H$ and $r_3 = k_3 C_{BP} C_{HP}$, respectively.

Assumptions for the model development

- The organic and aqueous phases are separately perfectly stirred, as explained in the previous section.
- A resistance film is considered at the two polymer sides and is represented by a "linear driving force" law.
- The polymer swelling is represented by a "linear driving force" law.
- The diffusions of species B and H through the polymeric membrane are described by the Fick's law.
- The organic phase volume V_A is considered to be constant during the reaction.

Figure 3 shows the processes taking place and the resulting concentration profiles, where the zones I, II, III, IV, and V represent the organic phase, the resistance film reaction zone, the polymer, the resistance film on the aqueous phase side, and the aqueous phase, respectively.

Model development

Considering the previous description, we develop the mass balances necessary to describe all the phenomena occurring during the experiment.

Swelling in the Polymer. When a liquid is absorbed and if the swelling is significant, the interface between the liquid and the polymer moves. This movement of the boundary complicates significantly the analysis of the process. Secondly, convective flows in the compartment polymer-solvent can be induced by mutual diffusion processes. Duda and Vrentas[18] and Alsoy and Duda[19] proposed a model to describe this process. The equations are solved thereafter for different conditions with the aim of elucidating the influence of these two phenomena on the process of sorption.

Some researchers consider that the swelling of dry polymer is not initially due to the diffusion of the solvent but to the capillarity.[20] In this case, the equation of Washburn is used and the permeability, the porosity of the polymer, and the densities and viscosities of the fluids will be taken into account to calculate the speed to which the polymer absorbs the solvent.[21]

Some analysis considers the sorption of liquid on a polymer is done by diffusion and not by capillarity.[19] The analysis is applicable also to desorption when a liquid or a vapor of low molar mass diffuses out of the polymer. In the model proposed by Alsoy and Duda,[19] the system is supposed to be isothermal with no reaction and only the swelling of a dry polymer is considered. Finally, to focus on the effects of the movement of the limit and the convection, the binary coefficient of diffusion is regarded as being independent of the concentration.[19] It is clear that starting from the equations developed by this model, the inclusion of the effects of the moving boundary and the convection induced by the diffusion, makes the resolution analysis extremely complicated and very few solutions of these equations were proposed. However, this problem can be formulated in a simpler form by using variables transformations.[18,19,21] The setting of the process of sorption in the system with the new coordinates is a partial derivative equation that has a standard form of the equation of the continuity of the species with an effective diffusivity according to the concentration.

In this article, we will use this transformation, but in our case the swelling and the reaction occur simultaneously. This transformation will be presented later on.

The variable $X(t) = (V_e/V_T)$ represents the porosity of the polymer; since the section of the reactor is constant, this is equivalent to giving:

$$X = \frac{(h_0 - h)}{e} \qquad (1)$$

We choose to represent its variation rate by the linear driving force model with constant coefficient V_g:

$$e\,\frac{dX}{dt} + X\,\frac{de}{dt} = V_g(X_{eq} - X) \qquad (2)$$

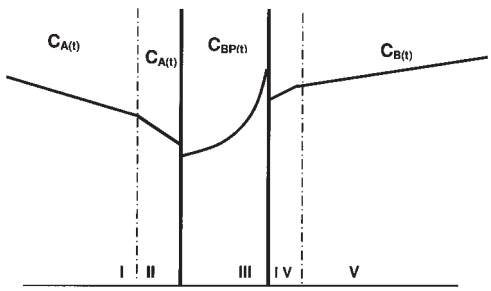

Figure 3. Concentration profiles resulting on monomer B diffusion and polymerization of A and B.

From now on, let us express the next balance equations with respect to the dimensionless variables:

$$C_B = \overline{C_B} C_{B0},\ C_A = \overline{C_A} C_{A0},\ C_{AS} = \overline{C_{AS}} C_{A0},\ C_{BP} = \overline{C_{BP}} C_{B0},$$
$$C_{HP} = \overline{C_{HP}} C_{B0},\ C_H = \overline{C_H} C_{B0}$$

Mass Balance of the Polymer. The apparent mass of the polymer is equal to the sum of the mass of the polymer produced by the reaction and the mass of the water due to the swelling. This approach requires the knowledge of the apparent mass density of the polymer ρ_{app}. The increase of the polymer thin film thickness during the reaction $e(t)$ considering water swelling is given by:

$$\frac{de}{dt} = \underbrace{\frac{M_p \lambda_p k_1}{\rho_{app}} C_{B0} C_{A0}^n \overline{C_{AS}^n} \frac{\overline{C_{BP}}}{X}}_{\text{due to the reaction}} + \underbrace{\frac{\rho_e}{\rho_{app}} \left(e \frac{dX}{dt} + X \frac{de}{dt} \right)}_{\text{due to the swelling}} \quad (3)$$

Mass Balance of the Monomer A in the Organic Phase. The variation of the mole number of monomer A due to the mass transfer between the organic phase and the resistance film is represented by a driving force law:

$$\frac{d\overline{C_A}}{dt} = \frac{k_A}{h_A} (\overline{C_{AS}} - \overline{C_A}) \quad (4)$$

Moreover, we suppose that the consumption of A by the reaction at the surface is instantaneous. From these two hypotheses we obtain the algebraic relation:

$$\overline{C_A} = \overline{C_{AS}} - \frac{\lambda_A k_1}{k_A} C_{B0} C_{A0}^{n-1} \overline{C_{AS}^n} \frac{\overline{C_{BP}}}{X} \quad (5)$$

Mass Balance of B and H in the Aqueous Phase. The dynamic behavior of concentration of the components B and H is governed by Eqs. 6 and 7, respectively:

$$\overline{C_B} \left(e \frac{dX}{dt} + X \frac{de}{dt} \right) + \frac{d\overline{C_B}}{dt} (h_0 - Xe) = k_B \left(\frac{\overline{C_{BP}}}{X} - \overline{C_B} \right) - \lambda_B k_3 \overline{C_B} C_{B0} \overline{C_H} \quad (6)$$

$$\overline{C_H} \left(e \frac{dX}{dt} + X \frac{de}{dt} \right) + \frac{d\overline{C_H}}{dt} (h_0 - Xe) = k_B \left(\frac{\overline{C_{HP}}}{X} - \overline{C_H} \right) - \lambda_B k_3 \overline{C_B} C_{B0} \overline{C_H} \quad (7)$$

Mass Balance of B in the Polymer Film. For this balance, the coordinate change previously mentioned appears, namely $\varphi(x, t) = (x/e(t))$. With this new variable, the expression of the mass balance is given by:

$$\frac{\partial \overline{C_{BP}}}{\partial t} = \frac{D_{BP}}{e^2} \frac{\partial^2 \overline{C_{BP}}}{\partial \varphi^2} - \varphi \frac{\partial e}{\partial t} \frac{\partial \overline{C_{BP}}}{e \partial \varphi} + \lambda_B k_3 \overline{C_{HP} C_{BP}} C_{B0} \quad (8)$$

Table 1. Calculated Parameters and Operating Conditions

	Calculated Parameters and Operating Conditions	(SI)
Calculated parameters	k_A	$1.7\ 10^{-2}$ m · s^{-1}
	k_B	$1.67\ 10^{-2}$ m · s^{-1}
	k_H	$3.4\ 10^{-4}$ m · s^{-1}
Operating conditions	C_{A0}	24.98 mol · m^{-3}
	C_{B0}	125.38 mol · m^{-3}
	C_{BP0}	0 mol · m^{-3}
	h_0	$7\ 10^{-2}$ m
	h_A	$3.2\ 10^{-2}$ m

This coordinate change introduces a new term $\varphi(\partial e/\partial t)(\partial \overline{C_{BP}}/e\partial\varphi)$ relative to the convection induced by the moving boundary $e(t)$.

The boundary conditions are given by:

$$\text{at } x = 0\ (\varphi = 0): \frac{\overline{C_{BP}}}{X} - \overline{C_{BP}} = \frac{D_{BP}}{e k_B} \frac{\partial \overline{C_{BP}}}{\partial \varphi} \quad (9)$$

$$x = e\ (\varphi = 1): \frac{de}{dt} \overline{C_{BP}} = \frac{D_{BP}}{e} \frac{\partial \overline{C_{BP}}}{\partial \varphi}\bigg|_{\varphi=1} + \lambda_B k_1 C_{A0}^n \overline{C_{AS}^n} \frac{\overline{C_{BP}}}{X} \quad (10)$$

Mass Balance of H in the Polymer Film. Similarly, the concentration of H in the polymer film with its boundary conditions is given by Eqs. 11, 12, and 13:

$$\frac{\partial \overline{C_{HP}}}{\partial t} = \frac{D_{HP}}{e^2} \frac{\partial^2 \overline{C_{HP}}}{\partial \varphi^2} - \varphi \frac{\partial e}{\partial t} \frac{\partial \overline{C_{BP}}}{e \partial \varphi} + \lambda_B k_1 \overline{C_{HP} C_{BP}} C_{B0} \quad (11)$$

$$\varphi = 0 \quad \frac{\overline{C_{HP}}}{X} - \overline{C_H} = \frac{D_{HP}}{e k_H} \frac{\partial \overline{C_{HP}}}{\partial \varphi} \quad (12)$$

$$\varphi = 1 \quad \frac{de}{dt} \overline{C_{HP}} = \frac{D_{HP}}{e} \frac{\partial \overline{C_{HP}}}{\partial \varphi}\bigg|_{\varphi=1} + \lambda_H k_1 \overline{C_{AS}^n} \frac{\overline{C_{BP}}}{X} \overline{C_{A0}^n} \quad (13)$$

Parameter estimation

The dimensionless formulation makes appear 11 parameter groups with many unknown physical parameters: $(M_p \lambda_p k_1/\rho_p) C_{B0} \bar{C}_{A0}^n$, $(\lambda_A k_1/k_A) C_{B0} C_{A0}^{n-1}$, $\lambda_B k_3 C_{B0}$, D_{BP}, k_B, X_{eq}, $\lambda_B k_1 C_{A0}^n$, D_{HP}, k_H, and $\lambda_H k_1 C_{A0}^n$. This number is too high with respect to the available measurements. So we set the mass transfer coefficients k_A, k_B, and k_H since some correlations[22] are available. Their values are given in Table 1, as well as some initial conditions. With this choice, the kinetic constant and the diffusion constant will be estimated precisely.

Moreover, λ_A and λ_B, as well as λ_H and n, are fixed to 1. This choice of stoichiometry of the condensation polymerization is validated by the experimental curve (see Figure 4) for the global mass balance in the stationary regime.

The above equations (Eqs. 1-13) are spatially approximated by using an orthogonal collocation method.[23] This approximation leads us to solve a set of algebraic differential equations with respect to time. The routines available in the IMSL library

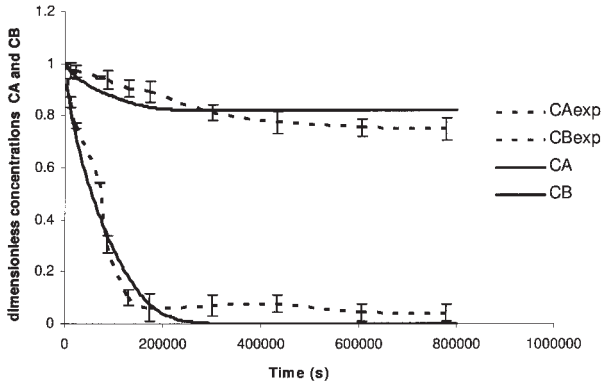

Figure 4. Monomers consumption: model prediction and experimental data.

(Visual Numerics) are used to solve the problem; the dynamical system is interpreted using the Petzold-Gear method (routine DASPG). An improvement is necessary since we have to use an interpolation routine (routine INTPR) to update the values of the state variables at the collocation points.[23] Because of the moving boundary problem, when the time is running, the collocation points do not represent the same spatial position.

The estimation procedure is based on the time domain fitting of the parameters: X_{eq}, k_3, k_1, V_g, D_{BP}, ρ_e/ρ_{app}, and M_p/ρ_{app}. The optimization is performed by a Levenberg-Marquard optimization procedure (subroutine DBCLSF of the IMSL library), and the criterion $J(\theta)$ to minimize with respect to the vector of parameters θ is the sum of the square difference between the experimental vector y_{mes} formed by the measures of C_A, C_B, and e for different times and the simulated one y_{model}. The optimization is made under the physical constraints that macroparameters are non negative $\theta \geq 0$:

$$J(\theta) = \min_{\theta \geq 0} \left(\sum \left(y_{\text{mes}}(t) - y_{\text{model}}(t) \right) \right)^2$$

Results and discussion

Polymer thickness due to the polymer formation and to the water sorption (e), monomers consumptions (C_B(t) and C_A(t)), and the water swelling were estimated and compared to experimental data (Figures 4 and 5).

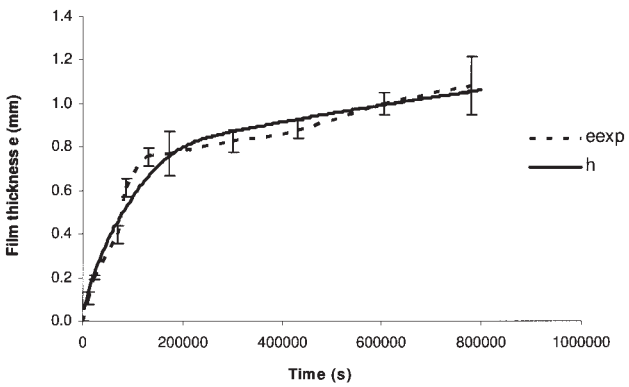

Figure 5. Polymer thickness: model prediction and experimental data.

Table 2. Estimated Parameters with Confidence Level at 95%

Estimated Parameters (θ)	(Value $\pm$ Precision)
X_{eq}	(0.671 $\pm$ 0.024)
k_3	(3.140 $\pm$ 0.048) 10^{-9} m$^3 \cdot$ s$^{-1} \cdot$ mol^{-1}
k_1	(1.099 $\pm$ 0.048) 10^{-8} m$^4 \cdot$ s$^{-1} \cdot$ mol^{-1}
V_g	(7.830 $\pm$ 0.098) 10^{-10} m $\cdot$ s^{-1}
D_{BP}	(3.270 $\pm$ 0.095) 10^{-10} m$^2 \cdot$ sl^{-1}
ρ_e/ρ_{app}	(0.950 $\pm$ 0.172)
M_p/ρ_{app}	(9.500 $\pm$ 0.165) 10^{-4} m$^3 \cdot$ mol

The monomers concentrations represented in Figure 4 are dimensionless with respect to their initial values. The condensation polymerizaton is achieved after 50 hours. The sebacoyl chloride (A) is totally consumed but not the diethylenetriamine (B), which remains in high concentrations when the reaction extinguishes. This study of the kinetic of the condensation polymerization is very significant; it enables us to know the duration of the reaction and to deduce that the reaction of interfacial polycondensation stops because the totality of sebacoyl chloride (A) is consumed.

Figure 5 shows the evolution of the polymer thickness according to time during the condensation polymerization. The thickness of the polymer membrane increases significantly between 0 and 50 hours corresponding to the polymer formation. After that time, the thickness still grows, but this evolution is due to the water sorption, the swelling.

The estimated parameters are given in Table 2.

The obtained parameters can be used to simulate the spherical model. The simulation of the spherical model permits obtaining the thickness of the polymer membrane and having knowledge about the swelling of this membrane. The consistency of this estimation is reinforced by the fact that the diffusion coefficient D_{BP} is in the same order as the one computed by the correlation given in Lieto[22]: $D_{BP} = 7.74\ 10^{-10}$ m^{2}s^{-1}. We conclude that the resistance of the membrane is low.

Spherical Model

Up to now, we have dealt with a planar geometry. We have proposed a model taking into account reaction and diffusion phenomena. On the basis of this model, we have estimated some important parameters. Let us now proceed with the spherical geometry model and reuse these parameters to simulate this new model.

The system considered here is the encapsulation of a dispersed organic phase using the interfacial polycondensation combined with spontaneous emulsification technique. The polymerization reaction takes place after total water miscible solvent diffusion.[24]

The interfacial polycondensation combined with spontaneous emulsification is a new technique for nanocapsules preparation. It is a one step procedure, where an organic phase composed of a water miscible solvent (acetone), lipophilic monomer (A), oil, and a lipophilic surfactant (Span® 85 with HLB = 1.81 at 25°C), is injected in an aqueous phase containing hydrophilic monomer (B) and the hydrophilic emulsifying agent (Tween® 20 with HLB = 16 at 25°C).

The water miscible solvent diffuses to the aqueous phase, the

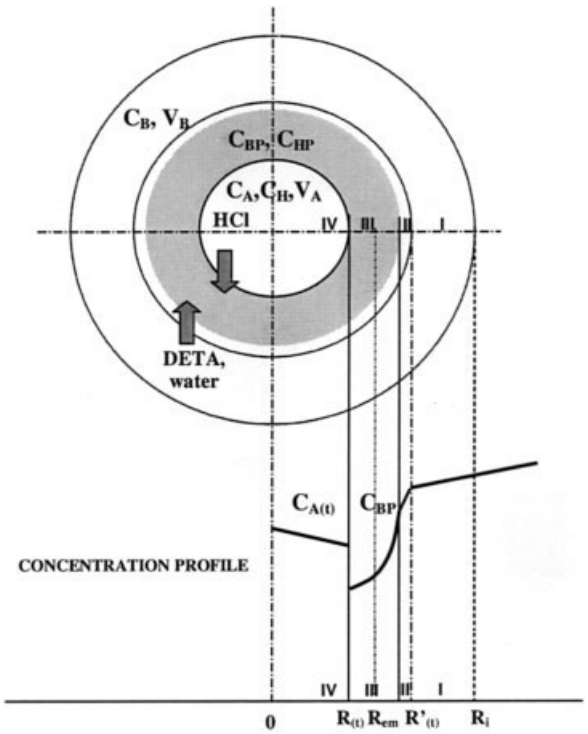

Figure 6. Representation of the spherical model at time t.

oil precipitates as droplets, and the two monomers react at the interface, forming a membrane around the nano emulsion leading to nanocapsules.[25]

Figure 6 gives the spherical representation of the different phases in presence and shows the different variables involved in the growing of the sphere. Moreover, on the bottom of the figure, a typical concentration profile is represented along the radial coordinate. Since the radius of the capsule varies with the time, the problem is again a moving boundary problem.

Until now, the process of encapsulation remains complex. In order to make easier the development of the model and its resolution, the following additional assumptions are made:

- Modeling is done on a population of identical particles of radius $R_i = 200$ nm.[25]
- The homogeneous polymer B is considered to diffuse towards the interior of the lately formed capsule and towards the zone of the reaction (R1). The standard profile of concentration versus time t is illustrated in Figure 6.
- The Fick's law is chosen to represent the diffusion.
- The polymerization reaction occurs after total diffusion of the solvent. $(R_{em} - R(t))$ results only from the condensation polymerization. $R(t)$ is the internal radius of the capsule.
- The external radius $R'(t)$ expands at the outside of the capsule. $(R'(t) - R_{em})$ results only from the swelling of the polymer. This evolution is due to the swelling (R2).
- The swelling is represented by a linear driving force.
- The resistance film is supposed only outside the sphere.

Finally, Figure 6 shows the four zones from I to IV involved in the process, namely, the aqueous phase, the film, the polymer, and the organic phase.

Model development

Let us consider the dimensionless concentrations as previously.

Mass Balance of B in the Aqueous Phase.

$$-\overline{C_B}\frac{dR'(t)}{dt} + \frac{(R_i^3 - R'^3(t))}{3R'^2(t)}\frac{d\overline{C_B}}{dt} = k_B(\overline{C_{BP}} - \overline{C_B}) + \lambda_B k_3 C_{B0}\overline{C_B C_H} \quad (14)$$

This equation is obtained with the same reasoning as previously. V_B representing the aqueous phase volume between the radius R_i and $R'(t)$: $V_B = \frac{4}{3}\pi R_i^3 - \frac{4}{3}\pi R'^3(t)$ is needed, as well its derivative, to express the concentration balance.

Mass Balance of H in the Aqueous Phase.

$$-\overline{C_H}\frac{dR'(t)}{dt} + \frac{(R_i^3 - R'^3(t))}{3R'^2(t)}\frac{d\overline{C_H}}{dt} = k_H\left(\frac{\overline{C_H}}{X} - \overline{C_{HP}}\right) + \lambda_B k_3 C_{B0}\overline{C_B C_H} \quad (15)$$

Mass Balance of A in the Polymer Phase. The volume of the capsule is equal to $V_A = \frac{4}{3}\pi R^3(t)$. From this expression and its derivative, one obtains:

$$\frac{R(t)}{3}\frac{d\overline{C_A}}{dt} + \overline{C_A}\frac{dR(t)}{dt} = \lambda_A k_1 \overline{C_{A(R(t))}C_{B(R(t))}}C_{B0} \quad (16)$$

Mass Balance of the Polymer. The polymer is only due to the reaction between the monomer A and the monomer B. The volume of the polymer, without the swelling, is given by the relation $V_P = \frac{4}{3}\pi R_{em}^3 - \frac{4}{3}\pi R^3(t)$. R_{em} is constant.

$$\frac{dR(t)}{dt} = -\frac{M_p}{\rho_{app}}\lambda_p k_1 C_{A0} C_{B0}\overline{C_{A(R(t))}C_{B(R(t))}} \quad (17)$$

Mass Balance of the Swelling. The total volume of the polymer film V_T represents the sum of the polymer formed by the reaction and the volume of water contained in the polymer. The volume corresponding to the swelling only is given by $V_e = \frac{4}{3}\pi R'^3(t) - \frac{4}{3}\pi R_{em}^3$, and the total volume by $V_T = \frac{4}{3}\pi R'^3(t) - \frac{4}{3}\pi R^3(t)$. With these formulas, the porosity X has the following expression:

$$X = \frac{R'^3(t) - R_{em}^3}{R'^3(t) - R^3(t)} \quad (18)$$

The variation of the water volume is given by Eq. 2 with the adequate surface. Replacing V_T and its derivative as well as the external surface of the sphere $S_{R'} = 4\pi R'^2(t)$, Eq. 2 has the following expression for the spherical geometry:

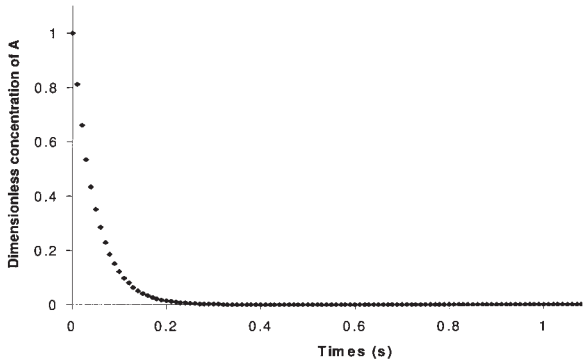

Figure 7. Concentration for monomer A for these operating conditions.

$$\frac{dR'(t)}{dt} = V_g\left(X_{eq} - \frac{R'^3(t) - R_{em}^3}{R'^3(t) - R^3(t)}\right) \tag{19}$$

Mass Balance of B in the Polymer. In order to write this mass balance in function of $R(t)$ and $R'(t)$, let us introduce the following coordinate transformation: $\varphi = (r - R(t)/R'(t) - R(t))$, where r is the radial coordinate ($r = 0$ at the center of the capsule). As previously, this coordinate change allows a simpler expression for the mass balance and boundary conditions and introduces a new term relative to convection induced by the moving boundaries $R(t)$ and $R'(t)$:

$$(R'(t) - R(t))\frac{\partial\overline{C_{BP}}}{\partial t} + \frac{\partial\overline{C_B}}{\partial\varphi}\left[\frac{-dR(t)}{dt} - \varphi\frac{d(R'(t) - R(t))}{dt}\right] = D_{BP}\frac{1}{\varphi(R'(t) - R(t)) + R(t)} \times \left[\frac{2\partial\overline{C_{BP}}}{\partial\varphi} + \frac{\varphi(R'(t) - R(t)) + R(t)}{R'(t) - R(t)}\frac{C_{B0}\partial^2\overline{C_{BP}}}{\partial\varphi^2}\right] \tag{20}$$

Boundary condition at $\varphi = 1$

$$-D_{BP}\frac{1}{R'(t) - R(t)}\left.\frac{\partial\overline{C_{B(R(t),t)}}}{\partial\varphi}\right|_{\varphi=1} = k_B\left(\left.\frac{\overline{C_{BP}}}{X}\right|_{\varphi-1} - \overline{C_B}\right) + \frac{dR'(t)}{dt}\overline{C_{BP(\varphi=1)}} \tag{21}$$

Boundary condition at $\varphi = 0$

$$-\frac{dR(t)}{dt}\overline{C_{BP(\varphi=0)}} - D_{BP}\frac{1}{R'(t) - R(t)}\left.\frac{\partial\overline{C_{BP}}}{\partial\varphi}\right|_{\varphi=0} = \lambda_B k_1 C_{A0}\overline{C_{A(\varphi=0)}}\left.\frac{\overline{C_{BP}}}{X}\right|_{\varphi=0} \tag{22}$$

Mass Balance of H in the Polymer (HP). With the same approach, we obtain:

$$(R'(t) - R(t))\frac{\partial\overline{C_{HP}}}{\partial t} + \frac{\partial\overline{C_{HP}}}{\partial\varphi}\left[\frac{-dR(t)}{dt} - \varphi\frac{d(R'(t) - R(t))}{dt}\right] = D_{BP}\frac{1}{\varphi(R'(t) - R(t)) + R(t)} \times \left[\frac{2\partial\overline{C_{HP}}}{\partial\varphi} + \frac{\varphi(R'(t) - R(t)) + R(t)}{R'(t) - R(t)}\frac{C_{B0}\partial^2\overline{C_{HP}}}{\partial\varphi^2}\right] \tag{23}$$

And for the boundary conditions at $\varphi = 1$

$$-D_{BP}\frac{1}{R'(t) - R(t)}\left.\frac{\partial\overline{C_{H(R(t),t)}}}{\partial\varphi}\right|_{\varphi=1} = k_B\left(\left.\frac{\overline{C_{HP}}}{X}\right|_{\varphi=1} - \overline{C_H}\right) + \frac{dR'(t)}{dt}\overline{C_{HP(\varphi=1)}} \tag{24}$$

and at $\varphi = 0$

$$-\frac{dR(t)}{dt}\overline{C_{HP(\varphi=0)}} - D_{BP}\frac{1}{R'(t) - R(t)}\left.\frac{\partial\overline{C_{HP}}}{\partial\varphi}\right|_{\varphi=0} = \lambda_H k_1 C_{A0}\overline{C_{A(\varphi=0)}}\left.\frac{\overline{C_{HP}}}{X}\right|_{\varphi=0} \tag{25}$$

Simulation and discussion

From a numerical point of view, the same method as previously is used to provide the simulation. For numerical purposes, the membrane thickness has to be fixed to a non zero initial value. The initial external radius of the nanocapsule and the initial internal one are chosen as $R'(0) = 200(1 + 10^{-6})$ nm and $R(0) = 200(1 - 10^{-5})$ nm, respectively; this corresponds to a thin membrane.

According to the correlations,[22] and thanks to the calculation of the diffusion coefficient made in the planar geometry, we obtain: $k_B = 0.774\ 10^{-2}$ m.s^{-1}, $k_H = 1.99\ 10^{-2}$ m.s^{-1}, and $k_A = 1.7\ 10^{-2}$m.s^{-1}. For this simulation, the following initial conditions are chosen as: $C_{AO} = 25$ mol m^3, $C_{BO} = 125.4$ mol m^{-3}, and $C_{BP0} = 0$.

Prediction of the Wall Thickness in the Spherical Case. The results obtained with these operating conditions are presented below: Figure 7 gives the profile of concentrations of A, and Figure 8 gives the evolution of the wall thickness.

The kinetic of the condensation polymerization is very fast.

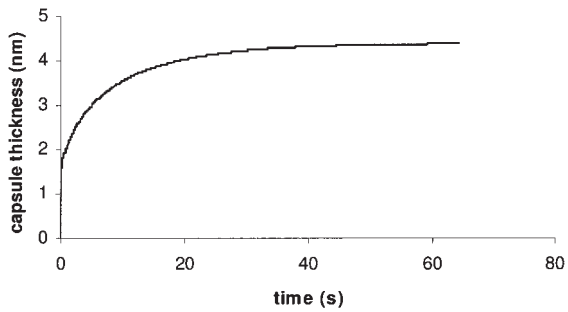

Figure 8. Thickness of the wall of the capsule versus time.

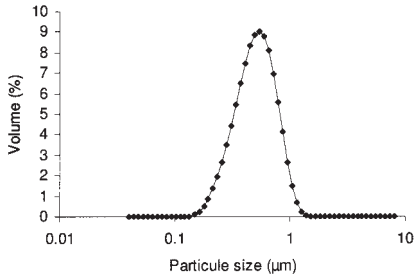

Figure 9. Capsule size distribution obtained from CS/DETA: mean radius 200nm.

The reaction stops after the overall consumption of sebacoyle chloride (0.2 s). After this time, the thickness increase is only due to the swelling. The time corresponding to the swelling is very important with respect to the reaction time (48.2 s). The final thickness of the capsule is estimated to 4.4 nm.

This result can be indirectly compared to experimental CSD obtained with using a light scattering particle size analyzer Coulter LS 230 (Beckman Coulter, Coultronics France). The mean radius is about 200nm, as shown in Figure 9. Knowing the initial quantities present in the experiment and making the assumptions that A is completely consumed, that the entire polymer is in the capsule membrane, and that there is no swelling, by a simple computation of mass balance with the use of the estimated parameter M_p/ρ_{app}, we finally obtain for a capsule of 200nm radius a wall thickness around 1.6nm. The result is clearly consistent with the model with swelling.

Moreover, this result is in the same order of magnitude as some observation done with the transmission electron microscopy (TEM) Topcon® EM002B, 200kV after negative staining technique on another polymer[25] having an equivalent molar mass with the same experimental conditions; that is to say, nanocapsules obtained using interfacial polymerization combined with spontaneous emulsification. The image corresponds to Figure 6 of [25] picture 3 page 97.

In the remaining part of the section, we present some simulation results showing the effect of initial conditions of the two monomers concentration on the concentration of A and on the thickness of the polymer film. Initially, the molar ratio [A]/[B] of the monomers is 1/10 (corresponding to the case treated above); the concentration of B is then modified, and the ratio of concentrations are: 1/15, 1/7, 1/5, and 1/2.5. In the second time, the initial concentration of A in the organic phase is changed: 0.6/10, 1/10, 1.2/10, 1.6/10, and 2/10.

Effect on the Consumption Kinetic of the Monomer A. The overall consumption of sebacoyle chloride informs us about the end of the interfacial polycondensation with the diethylenetriamine. The sebacoyle chloride is completely consumed after 1 s for a ratio [A]/[B] of 1/10. The kinetic of the interfacial polycondensation reaction in this case is very fast in comparison with the film model. In this work, the planar condensation polymerization stops after 50 hours, and 0.2 s for the nanocapsules. One thus expects that the kinetic in the case of microcapsules (average size around 600 μm) gives an intermediary time. The interfacial polycondensation reaction between an amine (Diethylenetriamine) and an acid chloride (TDC) is about 10 minutes according to the used initial concentrations[17] (12 minutes for $C_{B0} = 1\text{kmol.m}^{-3}$ and $C_{A0} = 0.23\ \text{kmol.m}^{-3}$).

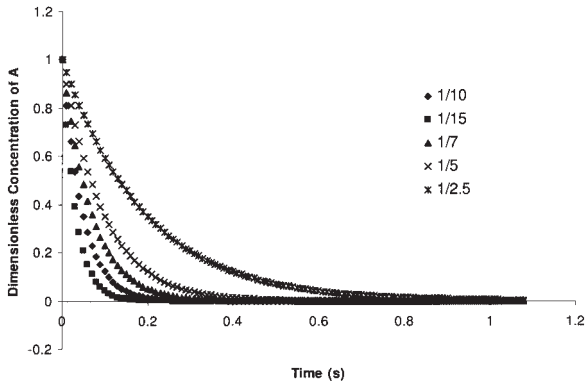

Figure 10. Concentration of the monomer A versus time for different initial concentration of B with fixed initial concentration of A (25 mol.m^{-3}).

The increase of the initial concentration of B (change of the molar ratio of 1/10 to 1/15) is at the origin of faster kinetic of consumption of A. On the contrary, the reduction in the initial concentration of B (change of the molar ratio of 1/10 to 1/2.5) is at the origin of a significant reduction of the consumption of A. However, the kinetic of the reaction remains fast and in one second the totality of A is consumed whatever its initial concentration, as shown in Figure 10.

If the initial concentration of monomer A varies, its kinetic of consumption remains very little unchanged. Indeed, according to Figure 11, the five curves corresponding to ratios 0.6/10, 1/10, 1.2/10, 1.6/10, and 2/10 are superimposed.

Effect of the Change of the Initial Concentrations of Monomers on the Thickness of the Membrane. According to Figure 12, the thickness of the capsule increases in the course of time until reaching a plateau from 40 s for different initial concentrations of A and fixed concentrations of B. According to the previous result, the condensation polymerization between the two monomers A and B stops after 0.2 s. The thickness corresponding to this time comes out only of this reaction.

The increase of the initial concentration of A of 25 mol.m^{-3} (molar ratio of 1/10) to 50 mol.m^{-3} (molar ratio of 2/10) is at the origin of an increase of the thickness of the capsule of 4.4 nm to 8.8 nm (Figure 12).

If the initial concentration of B varies, the thickness of the membrane of the capsule remains practically unchanged, con-

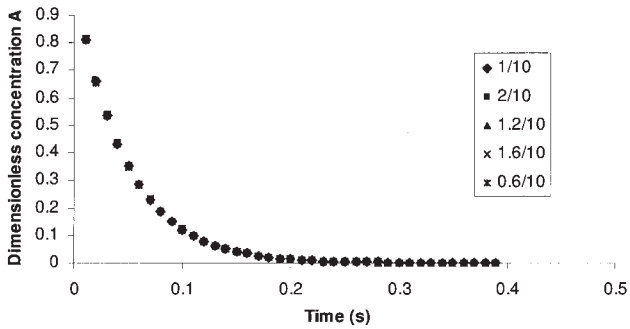

Figure 11. Concentration of the monomer A vs. time for different initial concentration of A with fixed initial concentration of B (125 mol.m^{-3}).

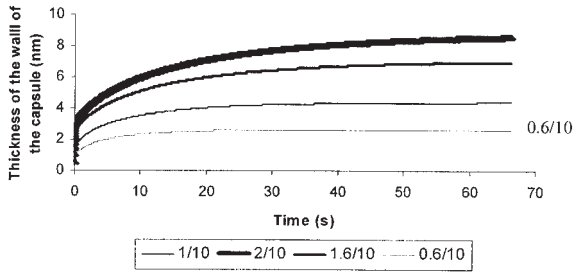

Figure 12. Thickness of the wall of the capsule versus time for various molar ratios with fixed initial concentration of B (125 mol.m^{-3}).

trary to the planar film model where the curves obtained with different molar ratios vary clearly. Only the curve obtained with a molar ratio of 1/10 is represented (Figure 11) because all the curves are merged. Clearly, the thickness of the membrane polymer is independent of the initial concentration of the monomer B. Indeed, when the value of C_{B0} changes, all the curves are superimposed.

These results indicate that the use of an initial high concentration in monomer A can significantly increase the thickening rate of the wall of the capsule. The maximum thickness of the wall of the membrane is thus limited by the initial concentration of A: C_{A0}. The initial concentration of B has effects only on the final time of reaction.

Conclusion

In this article, a planar model and a model for spherical nanocapsules have been developed. These models take into account the main phenomena occurring during the condensation polymerization: the swelling and the reaction. It appears that the swelling plays an important role in the thickness of the nanocapsule. The planar model is used in order to model the experimental reaction made in the reactor and to obtain measurements with good precision in order to estimate unknown parameters having effect in the process. The membrane appears to be very porous, the porosity being equal to 0.67 (X_{eq}). The diffusion coefficient of B in the polymer membrane is of the order of magnitude of the molecular liquid-liquid diffusion to within the porosity. From these results, we conclude that the polymer membrane does not offer resistance to the active principle but protects the latter.

The spherical dynamical model has been simulated by using the parameters estimated in the planar model. The spherical model is capable of predicting correctly the thickness of the membrane of the capsule; the operating conditions can be set in order to increase the membrane thickness and so to increase its protection role.

This work enables us to establish that the concentration of the Diethylenetriamine in the aqueous phase can be decreased. Moreover, the thickness of the membrane of the capsule can be controlled by changing this molar ratio of monomers.

Notation

A = sebacoyle chloride
B or DETA = diethylenetriamine
H = chloride acid
TDC = terephthaloyl dichloride

C_A = concentration of monomer A in the organic phase (mol.m^{-3})
C_{A0} = initial concentration of monomer A in the organic phase (mol.m^{-3})
C_{AS} = concentration of monomer A at the interface of the reaction in the organic phase (mol.m^{-3})
C_B = concentration of monomer B in the aqueous phase (mol.m^{-3})
C_{B0} = initial concentration of monomer B in the aqueous phase (mol.m^{-3})
C_{BP} = concentration of monomer B in the polymer (mol.m^{-3})
C_{BP0} = initial concentration of monomer B in the polymer (mol.m^{-3})
C_H = concentration of H at the interface of the reaction (mol.m^{-3})
C_{HP} = concentration of H in the polymer film (mol.m^{-3})
D_B = diffusion coefficient of monomer B in the aqueous phase (m^2.s^{-1})
D_A = diffusion coefficient of monomer A in the organic phase (m^2.s^{-1})
D_H = diffusion coefficient of H in the swelled polymer (m^2.s^{-1})
D_{BP} = diffusion coefficient of monomer B in the polymer film (m^2.s^{-1})
D_{HP} = diffusion coefficient of H in the polymer film (m^2.s^{-1})
e = thickness of the polymer film (m)
h_A = height of the organic phase (m)
h = height of the aqueous phase (m)
h_0 = initial height of the aqueous phase (m)
k_1 = rate constant (m^4.s^{-1}.mol^{-1})
k_3 = rate constant (m^3.s^{-1}.mol^{-1})
k_A = mass transfer coefficient of A in the organic phase (m.s^{-1})
k_B = mass transfer coefficient of B in the water (m.s^{-1})
k_H = mass transfer coefficient of H in the water (m.s^{-1})
M_p = molecular weight of the polymer (Kg.mol^{-1})
n = order of the reaction R1 with respect to A
r = radial coordinate (m)
R_{em} = initial external radius of the sphere (m)
R_i = fixed radius (m)
$R(t)$ = internal radius of the sphere (m)
$R'(t)$ = external radius of the sphere (m)
S_b = reactor section (m^2)
$S_{R'(t)}$, $S_{R(t)}$ = external surface of the sphere of radius, respectively, R′, R (m^2)
t = time (s)
V_A = volume of the organic phase (m^3)
V_B = volume of the aqueous phase (m^3)
V_e = water volume in the polymer (m^3)
V_{eq} = water volume in the polymer at equilibrium (m^3)
V_g = swelling rate of the polymer (m.s^{-1})
V_T = total volume of the polymer (m^3)
V_p = polymer volume formed by the reaction (m^3)
V_{Bp} = monomer B volume in the polymer (m^3)
X = porosity
X_{eq} = porosity at equilibrium porosity
λ_A, λ_B, λ_p = stoichiometric coefficient of monomer A, B, and polymer
λ_H = stoichiometric coefficient of H
ρ_{app} = apparent mass density of the polymer (Kg.m^{-3})
ρ_e = mass density of the water (Kg.m^{-3})

Literature Cited

1. Morgan PW, Kwolek SL. Interfacial polycondensation. II. Fundamentals of polymer formation at liquid interfaces. *J Polym Sci.* 1959;40: 299-327.
2. Morgan PW. *Condensation Polymers by Interfacial and Solution Methods.* New York: John Wiley & Sons, Inc.; 1965.
3. Morgan PW. Interfacial polymerization. Mark HF, Bikales NM, Overberger CG, Menges G, Kroschwits JI, Eds. *Encyclopedia of Polymer Science and Engineering, Vol. 8.* New York: John Wiley & Sons, Inc.; 1985.
4. Morgan PW. Development of low temperature polycondensation processes and aromatic polyamides. *J Polym Sci Polym Symp.* 1985;72: 27-37.
5. MacRitchie F. Interface effects on chemical reaction rate. Millich F, Carraher CE, Eds. *Interfacial Synthesis Fundamentals.* New York: Marcel Dekker; 1977:1.
6. Tsai HB, Lee YD. Polyarylates. I. Investigation of the interfacial

polycondensation reaction by UV. *J Polym Sci Part A: Polym Chem.* 1987;25:1505-1515.
7. Tsai HB, Lee YD. Polyarylates. III. Kinetic studies of interfacial polycondensation. *J Polym Sci Part A: Polym Chem.* 1987;25:2195-2206.
8. Kosky PG, Boden EP. The interfacial polycarbonate reaction: modelling the kinetics of carbamate side reactions. *J Polym Sci Part A: Polym Chem.* 1990;28:1507-1518.
9. Enkelmann V, Wegner G. Mechanism of interfacial polycondensation and the direct synthesis of polyamide membranes. *Appl Polym Symp.* 1975;26:365-372.
10. Pearson RG, Williams EL. Interfacial polymerization of an isocyanate and a diol. *J Polym Sci Part A: Polym Chem.* 1985;23:9-18.
11. Mikos AG, Kiparissides C. Skin formation in heterogeneous polymerization reactions. *J Membr Sci.* 1991;59:205-217.
12. Janssen LJJM, Te Nijenhuis K. Encapsulation by interfacial polycondensation. I. The capsule production and a model for wall growth. *J Membr Sci.* 1992;65:59-68.
13. Janssen LJJM, Te Nijenhuis K. Encapsulation by interfacial polycondensation. II. The membrane wall structure and the rate of the wall growth. *J Membr Sci.* 1992;65:69-75.
14. Janssen LJJM, Boersma A, Te Nijenhuis K. Encapsulation by interfacial polycondensation. III. Microencapsulation: the influence of process conditions on wall permeability. *J Membr Sci.* 1993;79:11-26.
15. Ji J, Dickson JM, Childs RF, McCarry BE. Mathematical model for the formation of thin-film composite membranes by interfacial polymerization: porous and dense films. *Macromolecules.* 2000;33:624-633.
16. Ji J, Mehta M. Mathematical model for the formation of thin-film composite hollow fiber and tubular membranes by interfacial polymerization. *J Membr Sci.* 2001;192:41-54.
17. Ji J, Childs RF, Mehta M. Mathematical model for encapsulation by interfacial polymerization. *J Membr Sci.* 2001;192:55-70.
18. Duda JL, Vrentas JS. Mathematical analysis of sorption experiments. *AIChE J.* 1971;17:464-469.
19. Alsoy S, Duda JL. Influence of swelling and diffusion-induced convection on polymer sorption processes. *AIChE J.* 2002;48:1849-1855.
20. Lago M, Araujo M. Capillary rise in porous media. *J Colloid Interface Sci.* 2001;234:35-43.
21. Crank J. *The Mathematics of Diffusion (2nd ed.)*. New York: Oxford University Press, Inc.; 1979.
22. Lieto J. Le génie chimique à l'usage des chimistes (2nd ed.). Paris: Lavoisier; 1998.
23. Villadsen J, Michelsen ML. *Solution of Differential Equation Models by Polynomial Approximation.* Int Series in Phys and Chem Engng Sci. Englewood Cliffs, NJ: Prentice-Hall; 1978.
24. Bouchemal K, Briançon S, Perrier E, Fessi H. Nano-emulsion formulation using spontaneous emulsification: solvent, oil and surfactant optimisation. *Int J Pharm.* 2004;280:241-251.
25. Bouchemal K, Briançon S, Perrier E, Fessi H, Bonnet I, Zydowicz. N. Synthesis and characterization of polyurethane and poly (ether urethane) nanocapsules using a new technique of interfacial polycondensation combined to spontaneous emulsification. *Int J Pharm*. 2004; 269:89-100.

Manuscript received May 19, 2005, and revision received Feb. 15, 2006.